ResearchGate

See discussions, stats, and author profiles for this publication at: https://www.researchgate.net/publication/45693915

pH-Tunable Ion Selectivity in Carbon Nanotube Pores

ARTICLE *in* LANGMUIR · SEPTEMBER 2010

Impact Factor: 4.46 · DOI: 10.1021/la101943h · Source: PubMed

CITATIONS
32

READS
89

8 AUTHORS, INCLUDING:

Francesco Fornasiero

37 PUBLICATIONS **776** CITATIONS

SEE PROFILE

Costas P. Grigoropoulos

University of California, Berkeley

295 PUBLICATIONS **7,013** CITATIONS

SEE PROFILE

Aleksandr Noy

Lawrence Livermore National Laboratory

133 PUBLICATIONS **6,745** CITATIONS

SEE PROFILE

Olgica Bakajin

Porifera Inc.

89 PUBLICATIONS **7,195** CITATIONS

SEE PROFILE

Available from: Aleksandr Noy
Retrieved on: 02 February 2016

Langmuir
Article
pubs.acs.org/Langmuir
© 2010 American Chemical Society

pH-Tunable Ion Selectivity in Carbon Nanotube Pores

Francesco Fornasiero,[†] Jung Bin In,[‡] Sangil Kim,[§] Hyung Gyu Park,[∥] Yinmin Wang,[†] Costas P. Grigoropoulos,[‡] Aleksandr Noy,[†,⊥] and Olgica Bakajin*[,§,#]

[†]*Physical and Life Sciences Directorate, Lawrence Livermore National Laboratory, Livermore, California 94550,* [‡]*Department of Mechanical Engineering, University of California at Berkeley, Berkeley, California 94720,* [§]*Porifera Inc., Hayward, California 94545,* [∥]*Institute of Energy Technology, Department of Mechanical and Process Engineering, ETH Zurich, Zurich, Switzerland,* [⊥]*School of Natural Sciences, University of California at Merced, Merced, California 95344, and* [#]*NSF Center for Biophotonics Science & Technology, University of California at Davis, Sacramento, California 95817*

Received May 14, 2010. Revised Manuscript Received July 19, 2010

The selectivity of ion transport in nanochannels is of primary importance for a number of physical, chemical, and biological processes ranging from fluid separation to ion-channel-regulated cellular processes. Fundamental understanding of these phenomena requires model nanochannels with well-defined and controllable structural properties. Carbon nanotubes provide an ideal choice for nanofluidic studies because of their simple chemistry and structure, the atomic scale smoothness and chemical inertness of the graphitic walls, and the tunability of their diameter and length. Here, we investigate the selectivity of single and, for the first time, binary salt mixtures transport through narrow carbon nanotubes that act as the only pores in a silicon nitride membrane. We demonstrate that negatively charged carboxylic groups are responsible for the ion rejection performance of carbon nanotube pores and that ion permeation of small salts can be tuned by varying solution pH. Investigation of the effect of solution composition and ion valences for binary electrolytes with common cation in a pressure-driven flow reveals that the addition of slower diffusing multivalent anions to a solution of faster diffusing monovalent anions favors permeation of the monovalent anion. Larger fractions and valences of the added multivalent anions lower the rejection of the monovalent anion. In some cases, we observe negative rejection at low monovalent ion content.

Introduction

Fluid confinement in pores with at least one dimension in the range of 1−100 nm often produces novel behavior because these pore sizes approach typical slip lengths, Debye lengths, and molecular dimensions.[1] The phenomena related to this nanoscale confinement are of significant scientific and technological interest since they may enable unique nanofluidic devices[2,3] as well as explain nanochannel-regulated biological processes. The past few years have seen an increasing attention toward understanding the behavior of ions in nanochannels[2,4−7] because of their implications for emerging areas such as nanoscale energy conversion,[8,9] nanofluidics transistors,[10−12] drug delivery,[13] and sensing[12,14,15] as well as in the more traditional fields of fluid separation, water purification, and desalination.[16] Also, nanochannel-regulated ion exchange across cellular membranes governs many important biological processes such as neural and muscle electrical signaling and cell homeostasis.[17] Despite the increasing theoretical and experimental effort, a complete understanding of the physics of ion behavior in nanochannels is still lacking. While the overwhelming majority of theoretical and experimental studies investigated the behavior of a single salt under nanoscale confinement, relevant ionic solutions for both biological processes[17] and nanotechnology applications[1,2] often consist of a mixture of several electrolytes. Ion interactions and unequal pore selectivity for the ions in the mixture may significantly affect ion partitioning and transport behavior in nanochannels. For example, variation of ionic composition modulates the electromotive force driving ion transport across cellular[17] and polymeric membranes;[1] small cation binding to the permeation sites may effectively block ion conductance in biological ion channels;[17] reversible switching of ion transport selectivity has been demonstrated in functionalized gold-nanotubule membranes by controlling solution pH.[5]

Clearly, availability of simple and well-defined nanochannels in a nanofluidic platform would be extremely useful to advance further the understanding and control of ion behavior at nanoscale. Carbon nanotubes (CNT) provide excellent nanochannels

*Corresponding author: tel (510) 695-2777; fax (510) 695-2775; e-mail olgica@poriferanano.com.

(1) Schoch, R. B.; Han, J. Y.; Renaud, P. *Rev. Mod. Phys.* **2008**, *80*, 839–883.
(2) Abgrall, P.; Nguyen, N. T. *Anal. Chem.* **2008**, *80*, 2326–2341.
(3) Sparreboom, W.; van den Berg, A.; Eijkel, J. C. T. *Nature Nanotechnol.* **2009**, *4*, 713–720.
(4) Ho, C.; Qiao, R.; Heng, J. B.; Chatterjee, A.; Timp, R. J.; Aluru, N. R.; Timp, G. *Proc. Natl. Acad. Sci. U.S.A.* **2005**, *102*, 10445–10450.
(5) Martin, C. R.; Nishizawa, M.; Jirage, K.; Kang, M. S.; Lee, S. B. *Adv. Mater.* **2001**, *13*, 1351–1362.
(6) Nishizawa, M.; Menon, V. P.; Martin, C. R. *Science* **1995**, *268*, 700–702.
(7) Scruggs, N. R.; Robertson, J. W. F.; Kasianowicz, J. J.; Migler, K. B. *Nano Lett.* **2009**, *9*, 3853–3859.
(8) Daiguji, H.; Yang, P. D.; Szeri, A. J.; Majumdar, A. *Nano Lett.* **2004**, *4*, 2315–2321.
(9) van der Heyden, F. H. J.; Bonthuis, D. J.; Stein, D.; Meyer, C.; Dekker, C. *Nano Lett.* **2007**, *7*, 1022–1025.
(10) Daiguji, H.; Yang, P. D.; Majumdar, A. *Nano Lett.* **2004**, *4*, 137–142.
(11) Karnik, R.; Fan, R.; Yue, M.; Li, D. Y.; Yang, P. D.; Majumdar, A. *Nano Lett.* **2005**, *5*, 943–948.
(12) Goldberger, J.; Fan, R.; Yang, P. D. *Acc. Chem. Res.* **2006**, *39*, 239–248.
(13) Schrlau, M. G.; Brailoiu, E.; Patel, S.; Gogotsi, Y.; Dun, N. J.; Bau, H. H. *Nanotechnology* **2008**, *19*.
(14) Liu, H. T.; He, J.; Tang, J. Y.; Liu, H.; Pang, P.; Cao, D.; Krstic, P.; Joseph, S.; Lindsay, S.; Nuckolls, C. *Science* **2010**, *327*, 64–67.
(15) Howorka, S.; Siwy, Z. *Chem. Soc. Rev.* **2009**, *38*, 2360–2384.
(16) Shannon, M. A.; Bohn, P. W.; Elimelech, M.; Georgiadis, J. G.; Marinas, B. J.; Mayes, A. M. *Nature* **2008**, *452*, 301–310.
(17) Hille, B. *Ion Channel of Excitable Membranes*, 3rd ed.; Sinauer Associates, Inc.: Sunderland, 2001; p 814.
(18) Noy, A.; Park, H. G.; Fornasiero, F.; Holt, J. K.; Grigoropoulos, C. P.; Bakajin, O. *Nano Today* **2007**, *2*, 22–29.

for nanofluidic studies[18−20] because of their very simple chemical composition and structure as well as the remarkable atomic scale smoothness and chemical inertness of their graphitic walls. In addition, CNTs share several common features with biological nanochannels,[18,20] such as the nanometer sized diameter, the hydrophobic inner pore wall, and an ultrafast water transport comparable to the flow rate reported for aquaporins.[21,22] Also, the easily functionalizabile CNT tip can be a facile target for localized chemical modifications to create a selective gate analogous to biological selectivity filters.[23−25] Thus, investigation of ionic flow in CNT channels will be extremely useful not only for the fundamental understanding of the physical mechanism underlying ion transport in synthetic nanopores but also for understanding much more structurally complex biological nanochannels.

Several molecular dynamics (MD) simulations have investigated ion transport, partitioning, and hydration for single salt solution in CNT pores.[26−39] The large majority of these studies consider subnanometer diameter CNTs, where size and confinement effects dominate. They show that ions encounter a large free energy penalty when entering nanochannels with diameter less than 0.8 nm because ion conduction requires partial stripping of the hydration shell. On the other hand, ions permeate easily through pores with dimensions larger than ∼1 nm. Simulations for single salt transport in structureless[40−42] and hydrophobic[43,44] model nanochannels and in boron nitride nanotubes[45] reach similar conclusions. For mixed salt solutions, MD studies of the small-ion selectivity in CNT pores are rare,[46] and no experimental report has been published.

Recently, we fabricated a simple and robust nanofluidic platform consisting of vertically aligned, sub-2 nm carbon nanotube pores spanning a gap-free silicon nitride (SiN) matrix,[21] and we employed this platform to demonstrate that CNTs are able to reject ions from dilute solutions while sustaining an extremely rapid water flow.[47] To understand ion behavior in nanoscale confinement, in this work we employ the same nanofluidic platform to investigate for the first time the transport of mixed electrolyte solutions through 0.8−2.6 nm wide carbon nanotubes (CNTs) under a pressure-driven flow. We measure the rejection of mixed electrolytes having common cations as a function of solution composition and of anion valence. Our results indicate that addition of more charged co-ions to the feed can significantly increase the permeation of less charged co-ions and lead in some cases to negative rejection. This effect is more pronounced at higher valence and larger concentration of the more charged co-ion and is probably due to a combined action of a Donnan exclusion mechanism and a strong diffusion potential. In addition, by varying solution pH, we unambiguously identify the chemical functionalities at the tip of CNTs that govern ion rejection through electrostatic interactions with the ions in solution. Measured pK_a of these groups matches closely that of carboxylic acids. These measurements demonstrate also that the control of solution pH enables tuning of ion permeability through carbon nanotube pores.

Results and Discussion

CNT Characterization. Carbon nanotube mats (Figure 1a) used for membrane fabrication were characterized by Raman spectroscopy and high-resolution transmission electron microscopy (TEM) imaging. Raman spectra of CNT arrays (Figure 1d) revealed well-graphitized CNT walls with a G/D band intensity ratio close to 10 and pronounced radial breathing modes. Also, a shoulder at ∼1570 cm^{-1} was clearly visible on the G band (1595 cm^{-1}). These features suggested the presence of a large SWNT and/or DWNT population. While the resolution of our TEM images could not clearly resolve the number of walls, a measured wall thickness < 3.5 Å confirmed that produced CNTs were SWNT and/or DWNT.[48,49] CNT diameter distribution measured by TEM imaging of about 40 CNTs (Figure 1b,c) spanned the interval 0.8−2.6 nm and peaks at ∼1.2 nm. The radial breathing modes indicated consistently the presence of 0.8−2.0 nm wide CNTs.

To investigate ion rejection for single and mixed salt solutions in these CNT pores, we drove the filtration of electrolyte solutions through a SiN/CNT membrane with a 0.69 bar pressure differential. After filtration, we separated the ionic species in both feed and permeate and measured their concentration by capillary electrophoresis (CE).

Single Salt Solutions. Measured rejection coefficients (Figure 2) of several salt solutions with the same equivalent concentration for three membranes (M1, M2, M3) indicate that their ion exclusion properties were comparable to those reported in Figure 4 of our previous publication[47] (membrane MP) for 1−2 nm wide double-walled CNT. Salts with the largest ratio of anion (z^-) vs cation (z^+) valence were excluded the most, in agreement with the prediction of Donnan equilibrium theory.

(19) Whitby, M.; Quirke, N. *Nature Nanotechnol*. **2007**, *2*, 87–94.
(20) Holt, J. K. *Adv. Mater*. **2009**, *21*, 1–9.
(21) Holt, J. K.; Park, H. G.; Wang, Y. M.; Stadermann, M.; Artyukhin, A. B.; Grigoropoulos, C. P.; Noy, A.; Bakajin, O. *Science* **2006**, *312*, 1034–1037.
(22) Majumder, M.; Chopra, N.; Andrews, R.; Hinds, B. J. *Nature* **2005**, *438*, 44–44.
(23) Majumder, M.; Zhan, X.; Andrews, R.; Hinds, B. J. *Langmuir* **2007**, *23*, 8624–8631.
(24) Nednoor, P.; Chopra, N.; Gavalas, V.; Bachas, L. G.; Hinds, B. J. *Chem. Mater*. **2005**, *17*, 3595–3599.
(25) Nednoor, P.; Gavalas, V. G.; Chopra, N.; Hinds, B. J.; Bachas, L. G. *J. Mater. Chem*. **2007**, *17*, 1755–1757.
(26) Nicholson, D.; Quirke, N. *Mol. Simul*. **2003**, *29*, 287–290.
(27) Liu, H. M.; Murad, S.; Jameson, C. J. *J. Chem. Phys*. **2006**, *125*, 14.
(28) Shao, Q.; Huang, L. L.; Zhou, J.; Lu, L. H.; Zhang, L. Z.; Lu, X. H.; Jiang, S. Y.; Gubbins, K. E.; Shen, W. F. *Phys. Chem. Chem. Phys*. **2008**, *10*, 1896–1906.
(29) Shao, Q.; Zhou, J.; Lu, L. H.; Lu, X. H.; Zhu, Y. D.; Jiang, S. Y. *Nano Lett*. **2009**, *9*, 989–994.
(30) Yang, L.; Garde, S. *J. Chem. Phys*. **2007**, *126*.
(31) Leung, K.; Rempe, S. B.; Lorenz, C. D. *Phys. Rev. Lett*. **2006**, *96*, 4.
(32) Sumikama, T.; Saito, S.; Ohmine, I. *J. Phys. Chem. B* **2006**, *110*, 20671–20677.
(33) Won, C. Y.; Aluru, N. R. *Chem. Phys. Lett*. **2009**, *478*, 185–190.
(34) Park, J. H.; Sinnott, S. B.; Aluru, N. R. *Nanotechnology* **2006**, *17*, 895–900.
(35) Joseph, S.; Mashl, R. J.; Jakobsson, E.; Aluru, N. R. *Nano Lett*. **2003**, *3*, 1399–1403.
(36) Corry, C. *J. Phys. Chem. B* **2008**, *112*, 1427–1434.
(37) Song, C.; Corry, B. *J. Phys. Chem. B* **2009**, *113*, 7642–7649.
(38) Hummer, G. *Mol. Phys*. **2007**, *105*, 201–207.
(39) Peter, C.; Hummer, G. *Biophys. J*. **2005**, *89*, 2222–2234.
(40) Carrillo-Tripp, M.; San-Roman, M. L.; Hernandez-Cobos, J.; Saint-Martin, H.; Ortega-Blake, I. In *Ion Hydration in Nanopores and the Molecular Basis of Selectivity*; 230th National Meeting of the American Chemical Society, Washington, DC, Aug 28−Sep 01, 2005; pp 243−250.
(41) Carrillo-Tripp, M.; Saint-Martin, H.; Ortega-Blake, I. *Phys. Rev. Lett*. **2004**, *93*.
(42) Tang, Y. W.; Chan, K. Y.; Szalai, I. *J. Phys. Chem. B* **2004**, *108*, 18204–18213.
(43) Beckstein, O.; Sansom, M. S. P. *Phys. Biol*. **2004**, *1*, 42–52.
(44) Beckstein, O.; Tai, K.; Sansom, M. S. P. *J. Am. Chem. Soc*. **2004**, *126*, 14694–14695.
(45) Hilder, T. A.; Gordon, D.; Chung, S. H. *Small* **2009**, *5*, 2183–2190.
(46) Liu, H. M.; Jameson, C. J.; Murad, S. In *Molecular Dynamics Simulation of Ion Selectivity Process in Nanopores*; Annual Meeting of the American Institute of Chemical Engineers, Salt Lake City, UT, Nov 09, 2007; pp 169−175.
(47) Fornasiero, F.; Park, H. G.; Holt, J. K.; Stadermann, M.; Grigoropoulos, C. P.; Noy, A.; Bakajin, O. *Proc. Natl. Acad. Sci. U.S.A*. **2008**, *105*, 17250–17255.
(48) Wei, J. Q.; Jiang, B.; Zhang, X. F.; Zhu, H. W.; Wu, D. H. *Chem. Phys. Lett*. **2003**, *376*, 753–757.
(49) Wei, J. Q.; Ci, L. J.; Jiang, B.; Li, Y. H.; Zhang, X. F.; Zhu, H. W.; Xu, C. L.; Wu, D. H. *J. Mater. Chem*. **2003**, *13*, 1340–1344.

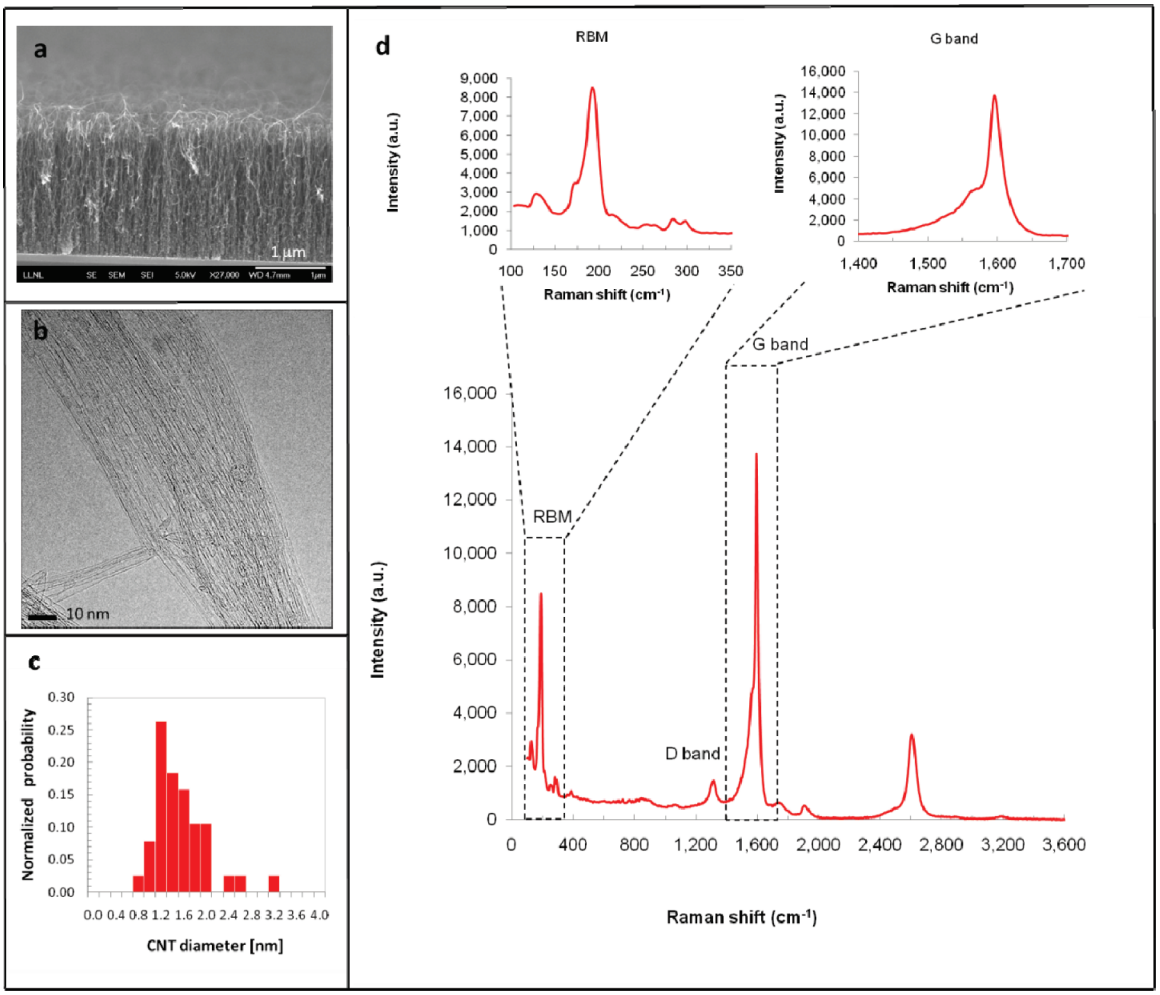

Figure 1. Characterization of CNT arrays: (a) a SEM image of a vertically aligned CNT array; (b) a representative TEM image used to determine the CNT diameter distribution shown in (c); Raman spectra for the full 100−3400 cm^{-1} range (d), for the radial breathing mode (inset on the left), and for the graphitic band (inset on the right) regions obtained with a 632.8 nm excitation laser.

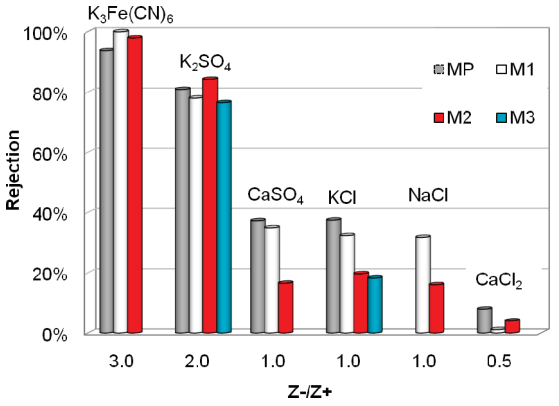

Figure 2. Rejection coefficients measured for four different membranes and six salt solutions with the same equivalent concentration but different ion valence. Gray bars are for membrane MP of a previous study;[47] white, red, and blue bars are for M1, M2, and M3 membranes of this work, respectively.

Also, salts with the same z^-/z^+ such as KCl, NaCl, and $CaSO_4$ experienced nearly identical rejection independent of charge and size of the constituent ions. However, some intermembrane differences existed. While membranes M1 and MP excluded all salt solutions in the same amount within experimental error, M2 and M3 were somewhat less selective for symmetrical salts KCl and $CaSO_4$.[50] Measured rejections for these salts were about 30−35% for M1 and 15−20% for M2 and M3. Because we grew separately each CNT array for membrane fabrication, and we etched each membrane individually to open the CNTs for ion permeation studies, we speculate that these differences may be due to small intermembrane variations of charge and/or pore size distribution during the fabrication process.

Mixed Electrolytes with Common Cations. *Monovalent−Divalent Mixtures.* To investigate how ion rejection was affected by the presence of a second ion with the same charge sign, we measured the rejection of binary KCl/K_2SO_4 salt solutions as a function of the solution composition while maintaining a constant K^+ concentration (Figure 3). For all three membranes M1, M2, and M3, sulfate ion rejection spanned the range of 70−80% and was rather insensitive to solution concentration within experimental accuracy. On the contrary, chloride rejection decreased steadily with its feed mole fraction, x_{Cl^-} (defined here as the molar ratio $Cl^-/(Cl^- + SO_4^{2-})$). While this decline in ion exclusion was only moderate for membrane M1 (from 35% at $x_{Cl^-} = 1.0$ to 17% at $x_{Cl^-} = 0.2$), we detected a crossover from positive to negative Cl^- rejection at $x_{Cl^-} \sim 0.5$ for M2 and M3 membranes. For $x_{Cl^-} <$ 0.5 the chloride concentration in the permeate was larger than in

(50) Because measured rejection for $CaCl_2$ is close to zero in all cases, measurements for this salt do not provide useful information for a membrane performance comparison.

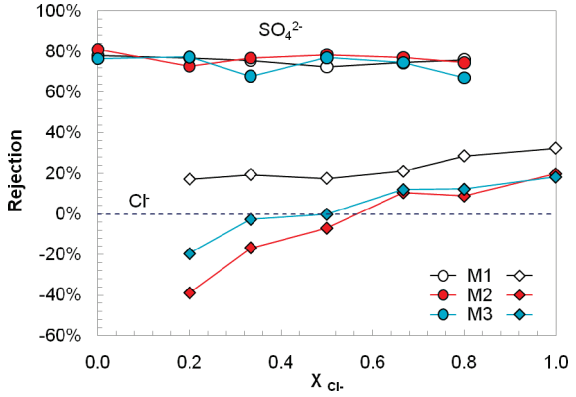

Figure 3. Rejection of binary KCl/K_2SO_4 salt solutions for three membranes as a function of the solution composition. Circles indicate SO_4^{2-} exclusion measurements while diamonds are for Cl^-. Data for M1, M2, and M3 membranes are labeled with white, red, and blue markers, respectively.

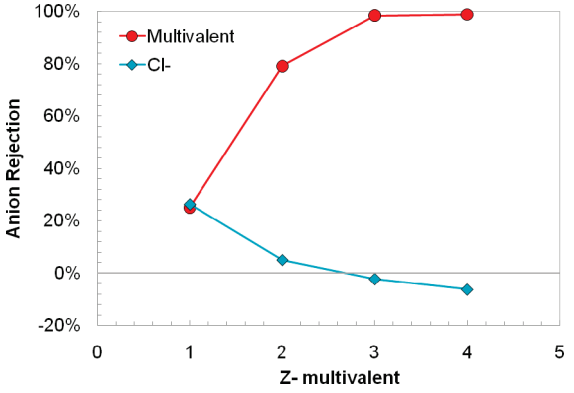

Figure 4. Dependence of Cl^- rejection (blue diamonds) on the co-ion valence. Larger co-ion valence produces a stronger co-ion rejection (red circles) and enhances the Cl^- permeation.

the feed; at $x_{Cl^-} = 0.2$, measured rejection was as low as −40% and −20% for M2 and M3, respectively, while, for a pure 1.0 mM KCl solution, chloride rejection approached 20% for both membranes. This different behavior of membrane M1 (no negative rejection) and membrane M2 and M3 (large negative rejection) may be also due to small intermembrane variations of charge and/or pore size distribution during fabrication. In particular, membranes M2 and M3 may have had a less charged surface and/or a wider pore size distribution.

Similar behavior has been observed for several polymeric nanofiltration membranes.[51−55] In agreement with our findings, an increase of the relative amount of multivalent ions decreased monovalent ion rejection. Also, multivalent ion rejection tends to slightly increase upon addition of monovalent ions. The Donnan membrane theory explains these trends qualitatively. In a mixture of electrolytes, counterions permeate easily through the membranes, while co-ions tend to be excluded by electrostatic repulsion. To maintain electroneutrality of the permeate solution, a fraction of the co-ions has to permeate as well. Because the monovalent co-ion experiences a weaker electrostatic repulsion than the multivalent co-ion, the former permeates preferentially with the counterions. For smaller mole fractions of the monovalent ions in the feed solution, a larger percentage of the monovalent ions has to permeate to maintain electroneutrality. The net result is a lower rejection of these ions.

Negative ion rejection of monovalent anions induced by the presence of multivalent anions is not unexpected.[51−60] For several polymeric nanofiltration membranes, both theoretical and experimental studies have reported negative rejection for monovalent co-ions in mixtures with divalent co-ions. Negative rejection occurs more frequently for "looser" or less charged membranes or when the applied pressure (and flow rate) is relatively low and the ion concentration is high, i.e., in less selective conditions.[61] Although Donnan equilibrium theory predicts the correct trend, it alone cannot explain the negative rejection; for a complete description of the phenomenon, the contribution of kinetic effects associated with convective, diffusion, and electromigration flow have to be accounted for.[60] In particular, a diffusion potential that prevents charge separation arises when the transport velocity of the anions differs from that of the cations in the membrane. When the anions are slower than the cations, the diffusion potential accelerates the anions toward the permeate side and vice versa.[62] If several co-ions of different mobilities are present in the feed, the diffusion potential maintains a zero electric current by assuming an intermediate strength that over-accelerates the more mobile co-ions and under-accelerates the less mobile co-ions. Thus, addition of large relative amounts of a slow, multivalent anion (such as SO_4^{2-}, bulk diffusivity $D_- = 1.065 \times 10^{-9}$ m^2/s)[63] in a solution containing fast monovalent anions (Cl^-, $D_- = 2.032 \times 10^{-9}$ m^2/s)[63] and cations (K^+, $D_+ = 1.956 \times 10^{-9}$ m^2/s)[63] gives rise to a strong diffusion potential that drives preferentially the fast monovalent anions toward the filtrate. Simultaneously, the less charged co-ions are less excluded by the membrane phase than the multivalent co-ions according to Donnan theory. Because electromigration and convective flow are both directed toward the permeate, this combination of strong driving force and not too reduced concentration in the membrane phase can result in negative rejection for the less-charged, fast co-ion.[60]

Sensitivity of Monovalent Co-Ion Rejection on the Valence of Added Co-Ions. The mechanism discussed in the previous section for an enhanced permeation of the less-charged co-ion induced by the presence of a more charged co-ion suggests that the addition of slower co-ions of higher valence (z_2) should result in a larger drop of monovalent co-ion exclusion. Indeed, for larger z_2, Donnan theory predicts an easier permeation of monovalent co-ion, which, coupled with the concomitant stronger diffusion potential, may lead to negative rejection. Our experimental results confirmed the expected trend (Figure 4). When we mixed KCl solution with KBr (Br^- bulk diffusivity at infinite dilution $D_- = 2.084 \times 10^{-9}$ m^2/s),[63] K_2SO_4 (SO_4^{2-} $D_- = 1.065 \times 10^{-9}$ m^2/s),[63] $K_3Fe(CN)_6$ ($Fe(CN)_6^{3-}$ $D_- = 0.896 \times 10^{-9}$ m^2/s),[63] and 1,3,6,8-pyrenetetrasulfonic acid tetrasodium salt ($PTSNa_4$; PTS^{4-}

(51) Bowen, W. R.; Mukhtar, H. *J. Membr. Sci.* **1996**, *112*, 263–274.
(52) Garcia-Aleman, J.; Dickson, J.; Mika, A. *J. Membr. Sci.* **2004**, *240*, 237–255.
(53) Garcia-Aleman, J.; Dickson, J. M. *J. Membr. Sci.* **2004**, *239*, 163–172.
(54) Tsuru, T.; Urairi, M.; Nakao, S.; Kimura, S. *Desalination* **1991**, *81*, 219–227.
(55) Tsuru, T.; Urairi, M.; Nakao, S.; Kimura, S. *J. Chem. Eng. Jpn.* **1991**, *24*, 518–524.
(56) Dey, T. K.; Ramachandhran, V.; Misra, B. M. *Desalination* **2000**, *127*, 165–175.
(57) Gilron, J.; Gara, N.; Kedem, O. *J. Membr. Sci.* **2001**, *185*, 223–236.
(58) Hagmeyer, G.; Gimbel, R. *Sep. Purif. Technol.* **1999**, *15*, 19–30.
(59) Wang, K. Y.; Chung, T. S. *J. Membr. Sci.* **2005**, *247*, 37–50.
(60) Yaroshchuk, A. E. In *Negative Rejection of Ions in Pressure-Driven Membrane Processes*; 33rd Conference on Membrane Electrochemistry, Krasnodar, Russia, May, 2007; Elsevier Science B.V.: Krasnodar, Russia, 2007; pp 150−173.
(61) Ion rejection increases by increasing applied pressure because the water flux is more sensitive to the pressure driving force than the ionic flux; it decreases for more concentrated salt solutions because of the increased osmotic pressure and increased driving force for salt diffusion.
(62) Osada, Y.; Nakagawa, T. *Membrane Science and Technology*. Marcel Dekker Inc.: New York, 1992.
(63) Newman, J.; Thomas-Alyea, K. E. *Electrochemical Systems*, 3rd ed.; John Wiley & Sons, Inc.: Hoboken, NJ, 2004; p 647.

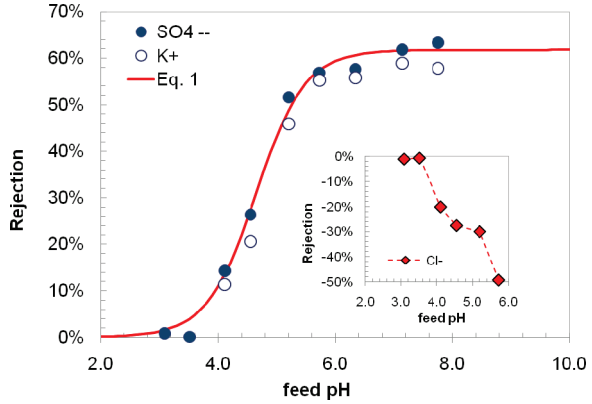

Figure 5. Effect of pH on measured rejection for a 0.5 mM K_2SO_4 solution. Filled circles indicate SO_4^{2-} rejection, while empty circles are for K^+. A fit to experimental SO_4^{2-} rejection with eq 1 and eq 2 (red line) gives a $pK_a = 4.8$ for the charged groups governing ion rejection in our CNT membranes. Inset: red diamonds show the negative rejection of the Cl^- introduced as HCl to adjust pH.

$D_- = 0.298 \times 10^{-9}$ m^2/s)[64] solutions while keeping constant both total cation concentration and Cl^- anion mole fraction ($x_{Cl^-} = 1/3$), the chloride rejection decreased monotonically from 26.4% for Br^- co-ions to −6.2% for PTS^{4-} co-ions. For this CNT membrane, the crossover between positive and negative rejection occurred between $z_2 = 2$ and $z_2 = 3$. Consistent with previous findings, Br^- exclusion matched Cl^- rejection within experimental accuracy (both KCl and KBr have identical z^-/z^+ ratio and similar diffusion coefficient).

Modulation of Ion Rejection by Solution pH. In a previous report[47] we demonstrated that ion rejection is dominated by electrostatic interactions between ions in solution and negatively charged groups at the membrane surface and that size effects are negligible. Because of the oxidation step used to open the CNTs, we expect that these charged functionalities are the ionized carboxylic groups at the CNT pore entrance. This claim is supported by a previous measurement of exclusion characteristics for CNT membranes at two different solution pH values, 3.8 and 7.2, one above the pK_a of the COOH group and one below it: as the solution pH changed from the high to the low value, the ion rejection dropped from 96% to 60% for a 0.5 mM $PTSNa_4$ salt solution.[47] However, other ionizable groups may be present on the silicon nitride surface, such as amphoteric −SiOH and basic $-SiNH_2$, $-Si_2NH$, $-Si_3N$, etc.,[65,66] which also may contribute to ion exclusion.[67] To establish unambiguously that COO^- groups are indeed responsible for the ion exclusion characteristics of our membranes, we monitored the rejection of a 0.5 mM K_2SO_4 solution as a function of pH in the pH range 3.0−8.0,[68] and we compared the results with a simple theory that allowed determination of the pK_a of the ion-rejecting surface charges. Note that, at 0.5 mM solution concentration, K_2SO_4 exclusion was close to its maximum value and nearly independent of small variation of ion concentrations and of solution Debye length upon addition of HCl or NaOH for pH adjustments. Recorded ion rejection for both SO_4^{2-} and K^+ ions was ∼60% and nearly constant for a pH > 5.5, but then dropped sharply to negligible exclusion by decreasing the pH from 5.5 to 3.5, and remained close to zero for more acidic pHs (Figure 5). For single salt solution, Donnan membrane equilibrium theory gives a simple analytical expression of the dependence of ion rejection on membrane charge, c_x^m, according to[69]

$$R = 1 - \frac{c_i^m}{c_i} = 1 - \left(\frac{|z_i| c_i}{|z_i| c_i^m + c_x^m} \right)^{|z_i/z_j|} \quad (1)$$

where c_i and c_i^m are the concentrations of co-ions in the solution and in the membrane phase, respectively, z is the ion valence, and subscripts i and j indicate co-ions and counterions, respectively. The variation of the membrane charge with solution pH follows the titration equation:

$$c_x^m = c_{x,0}^m \frac{10^{-pK_a}}{10^{-pK_a} + 10^{-pH}} \quad (2)$$

where $c_{x,0}^m$ is membrane charge when all functional groups responsible for ion rejection are fully ionized. By fitting pK_a (and $c_{x,0}^m$) to experimental ion rejections with eqs 1 and 2, we tested whether the data fit this simple picture of charged based ion selectivity. Fitted pK_a was equal to 4.8, very close to the $pK_a = 4.5$ of carboxylic groups on a carbon nanotube tip.[70,71] These results strongly suggest that, for our CNT membranes, the surface negative charges determining ion exclusion are ionized carboxylic groups at the CNT pore opening. Other negatively charged groups on the membrane matrix, such as ionized silanols, do not appear to influence ion rejection. Because no K_2SO_4 rejection was observed for pH < 3.5, i.e., when the carboxylic groups were completely protonated and electrostatic interactions were turned off, our results confirmed that no other mechanisms (e.g., size/hydrodynamic effects) contribute significantly to ion exclusion of small salts by 0.8−2.6 nm wide CNT pores. A direct consequence of these findings is that we can control ion transport through CNT pores from complete permeation to large exclusion by modulating CNT-tip charges with pH.

To lower K_2SO_4 solution pH, we added a few microliters of an HCl solution; thus, we introduced small amounts of a monovalent anion, Cl^-, in a solution of a divalent anion (SO_4^{2-}). At slightly acidic pHs, measured rejection for added chloride anions was strongly negative (inset in Figure 5). Indeed, in these conditions, the amount of Cl^- ions was very small with respect to the sulfate concentration, and the highly rejected sulfate ions produced a strong membrane potential. Following addition of larger amounts of HCl, more sulfate ions were able to permeate the membrane because of a reduced membrane charge; simultaneously, the ratio of Cl^-/SO_4^{2-} ions in solution increased and the membrane potential got weaker. As a consequence, proportionally less Cl^- ions permeated through the membrane to maintain charge balance, and recorded Cl^- exclusion increased in agreement with the results of the previous section. Finally, when all carboxylic groups were protonated and neutral, we measured no rejection for both Cl^- and SO_4^{2-} anions.

Conclusions

For the first time, we have investigated the ion selectivity of narrow CNT pores for small-ion mixtures. We have demonstrated

(64) Nagai, Y.; Unsworth, L. D.; Koutsopoulos, S.; Zhang, S. *J. Controlled Release* **2006**, *115*, 18–25.
(65) Cerovic, L. S.; Milonjic, S. K.; Bahloul-Hourlier, D.; Doucey, B. *Colloids Surf., A* **2002**, *197*, 147–156.
(66) Nakamatsu, T.; Saito, N.; Ishizaki, C.; Ishizaki, K. *J. Eur. Ceram. Soc.* **1998**, *18*, 1273–1279.
(67) Albeit discrepancies are present in the literature, most of reported values of point of zero charge correspond to a pH in the range 5.5−8.5 for a silicon nitride surface.[65]
(68) The pHs reported here are averages between the feed pH at the beginning of the filtration and at the conclusion of the experiment.
(69) Schaep, J.; Van der Bruggen, B.; Vandecasteele, C.; Wilms, D. *Sep. Purif. Technol.* **1998**, *14*, 155–162.
(70) Wong, S. S.; Joselevich, E.; Woolley, A. T.; Cheung, C. L.; Lieber, C. M. *Nature* **1998**, *394*, 52–55.
(71) Wong, S. S.; Woolley, A. T.; Joselevich, E.; Cheung, C. L.; Lieber, C. M. *J. Am. Chem. Soc.* **1998**, *120*, 8557–8558.

that ion rejection of monovalent co-ions by 0.8−2.6 nm wide CNTs is strongly affected by the presence of multivalent co-ions in solutions. Specifically, an increase of multivalent co-ion mole fraction favors the permeation of monovalent co-ions and may lead, in some cases, to monovalent-ion negative rejection. This effect is stronger for larger multivalent co-ion valences and can be explained on the basis of a Donnan exclusion mechanism coupled with the action of a strong diffusion potential across the CNT membrane. The phenomenon of negative rejection can potentially be exploited to separate multivalent and monovalent co-ions from a mixed salt solution at the ultrafast flow rates supported by CNT membranes.[21,22]

By modulating the solution pH, we have also demonstrated that carboxylic groups on the CNT tips most likely are the charged groups governing the ion rejection properties of our CNT membranes. Because ion exclusion is determined almost exclusively by an electrostatic mechanism for small ions in 0.8−2.6 nm wide CNT pores, control of the solution pH and, thus, of the membrane charge enables tuning ion permeation in a wide range, from strong exclusion to unimpeded transport.

These results may be useful for a variety of applications such as the design of nanofluidic systems based on CNT channels or the fabrication of highly efficient membranes for water purification as well as for elucidating the mechanism of ion transport and selectivity of biological nanopores.

Experimental Section

Materials. The following salts have been used in this study: potassium ferricyanide ($K_3Fe(CN)_6$, 99+% purity, Aldrich, St. Louis, MO), potassium chloride (KCl, 99.999%, Aldrich), potassium bromide (KBr, FTIR grade, International Crystal Laboratories, Garfield, NJ), potassium sulfate (K_2SO_4, 99%, Sigma, St. Louis, MO), calcium sulfate dihydrate ($CaSO_4$, 98%, Sigma), calcium chloride ($CaCl_2$, 99.5%, EM Science, Darmstadt, Germany), Fluka, Buchs, Switzerland), 1,3,6,8-pyrenetetrasulfonic acid tetrasodium salt ($PTSNa_4$, Invitrogen, Carlsbad, CA). All salt solutions and buffers are prepared using 18 MΩ water generated by a Milli-Q laboratory water purification system (Millipore, Bedford, MA) or double distilled water. All solutions are filtered through a 0.1 μm PVDF filter (Millipore) before use.

CNT Growth. A dense, vertically aligned array of carbon nanotubes with sub-2.6 nm diameters is grown at 850 °C by atmospheric-pressure catalytic chemical vapor deposition (CVD) on the surface of a 1 × 1 cm, 300 μm thick, prepatterned silicon (100) chip using ethylene as carbon source. The catalyst for CNT growth consists of 5 Å Fe/2 Å Mo bilayer deposited by electron beam evaporation and separated from the supporting Si wafer by a sputtered 30 nm Al_2O_3 barrier layer. After annealing the catalyst in a reducing environment (515 sccm argon, 400 sccm hydrogen) for 12 min at 850 °C, the hydrogen flow rate is reduced to 15 sccm and ethylene is introduced into the horizontal quartz tube reactor (22 mm i.d.) at 100 sccm. SWNT/DWNT forests are grown to a height between 3 and 7 μm.

Membrane Fabrication. With the exception of the CNT growth conditions, silicon nitride/CNT composite membranes were fabricated according to the previously reported method.[21] Briefly, vertically aligned carbon nanotubes are conformably encapsulated into a gap-free silicon nitride matrix by a low-pressure deposition process. The catalyst particles at the CNT root are removed by argon ion beam milling. Reactive ion etching in oxygen containing plasma removes excess silicon nitride on both sides of the membrane and opens the carbon nanotubes. The final result is a silicon nitride membrane with CNT pores that span the entire membrane thickness. The free-standing membrane area is ~0.175 mm^2 with a CNT density of about 2.5×10^{11} cm^{-2}.[21]

Raman Spectroscopy and Transmission Electron Microscopy. Raman spectra were collected with a Nicolet Almega XR dispersive Raman spectrometer (Thermo Scientific) at a 632.8 nm HeNe excitation laser (1.96 eV). Every Raman measurement was conducted at room temperature, and the laser power levels were kept at 1% (0.1 mW) to avoid excessive heating and subsequent CNT damage. A 100× objective lens was used to focus the laser beam on a 0.6 μm spot of the CNT forest for a 16 s acquisition time. TEM images were obtained using a Philips CM300-FEG TEM, operated at 300 kV with a 4.2 keV extraction voltage for the field-emission gun. CNTs were dry-deposited on a TEM copper grid with a lacey Formvar/carbon supporting film by using a press-printing method.

Nanofiltration Experiments. Filtration cell and protocols for the nanofiltration experiments and capillary electrophoresis (CE) analysis are described in detail elsewhere.[47] Briefly, 2 mL of feed salt solution is pressurized at 0.69 bar through a CNT membrane with a controlled nitrogen gas line, while the permeate is at atmospheric pressure. After 150−200 μL of solution has permeated through the CNT membrane, samples from both feed and permeate are collected for subsequent analysis by capillary electrophoresis (Hewlett-Packard 3D CE system, Agilent Technologies, Santa Clara, CA). Rejection coefficients are obtained from the ratio of peak areas of the corresponding ions in the CE chromatogram for permeate and feed samples. Permeate flow rate is measured as height variation of the column of salt solution in the feed chamber with respect to time. To study the pH sensitivity of ion rejection, the pH of a 0.5 mM K_2SO_4 feed solution is adjusted by adding a few microliters of hydrochloric acid (HCl) or sodium hydroxide (NaOH) solutions. The added base or acid for pH adjustment has minor impact on ionic strength, osmotic pressure, and Debye length except at the lowest pH (3.0) considered in this study. For the binary KCl/K_2SO_4 salt experiments and for the mono/multivalent anion mixture experiments, appropriate amounts of corresponding single-salt stock solutions are mixed to obtain a total anion (cation) equivalent concentration equal to 1.0 mM.

Experiments Testing Rejection Sensitivity to Co-Ion Valence. Except for PTS^{4-} ion concentration is obtained by capillary electrophoresis as explained above. For PTS^{4-} the UV spectrum is obtained with a Lambda 25 UV−vis spectrometer (PerkinElmer, Waltham, MA) after a 1:20 dilution with 18 MΩ water. PTS^{4-} concentration is measured at 244, 283, and 375 nm. Measured anion rejection coefficients are independent of the chosen wavelength.

Acknowledgment. This project received partial support from the Defense Threat Reduction Agency-Joint Science and Technology Office for Chemical and Biological Defense (Grant BRBAA07-F-1-0066) and from Lawrence Livermore National Laboratory. Lawrence Livermore National Laboratory is operated by Lawrence Livermore National Security, LLC, for the U.S. Department of Energy, National Nuclear Security Administration under Contract DE-AC52-07NA27344. A.N., C.G., S.K., J.B.I., and O.B. acknowledge support by NSF NIRT CBET-0709090. F.F. acknowledges support by DTRA (BB08PRO053 project). O.B. and S.K. acknowledge support by DARPA DSO. O.B. also acknowledges support by the Center for Biophotonics, a NSF Science and Technology Center, managed by the University of California, Davis, under Cooperative Agreement PHY 0120999.